Bioconjugate Chemistry

Article

pubs.acs.org/bc

# Complete Structural Elucidation of an Oxidized Polysialic Acid Drug Intermediate by Nuclear Magnetic Resonance Spectroscopy

G. Joseph Ray,[†] Neil Ravenscroft,[‡] Jürgen Siekmann,[§] Zhenqing Zhang,[∥] Paul Sanders,[†] Umesh Shaligram,[⊥] Christina M. Szabo,*[,†] and Paul Kosma[#]

[†]Baxter Healthcare Corporation, Round Lake, 60073, Illinois, United States

[‡]Department of Chemistry, University of Cape Town, Rondebosch 7701, South Africa

[§]Baxter Innovations GmbH, Vienna, A-1221, Austria

[∥]College of Pharmaceutical Science, Soochow University, Suzhou, Jiangsu Province, P. R. China, 215123

[⊥]Serum Institute of India, Ltd., Hadapsar, Pune, 411028, Maharashtra, India

[#]Department of Chemistry, University of Natural Resources and Life Sciences, Vienna, A-1190, Austria

Supporting Information

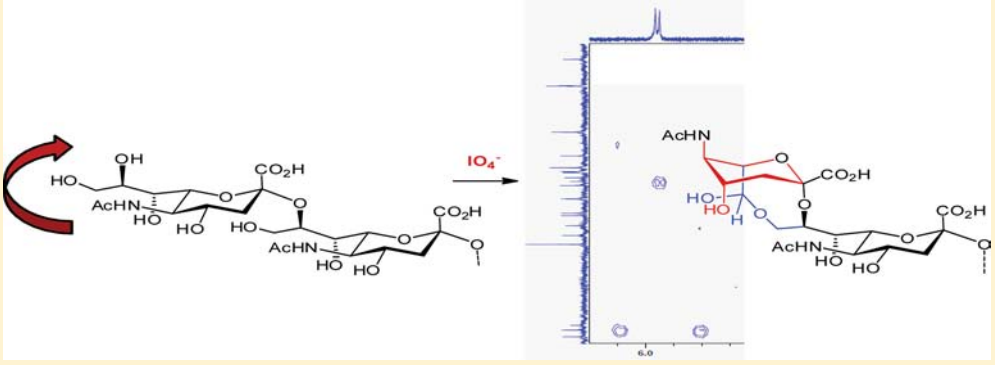


**ABSTRACT:** Polysialic acid (PSA) is a high molecular weight glycan composed of repeat units of α(2→8) linked 5-*N*-acetyl-neuraminic acid. Mild periodate oxidation of PSA selectively targets the end sialic acid ring containing three adjacent alcohols generating a putative aldehyde, which can be used for terminal attachment of PSA to therapeutic proteins. The work presented here permitted complete NMR peak assignments of not only the repeat units, but also the two terminal units at each end of oxidized PSA, an intermediate, which can be used to improve drug performance. The assignments were made using a variety of NMR techniques on oligomers of sialic acid as well as oxidized PSA with molecular masses of 4 and 20 kDa. This enabled structure elucidation that showed the actual moiety formed was not the expected aldehyde or its hydrate, but is a hemiacetal between the oxidation site on the terminal sialic acid ring and the penultimate ring. The existence of a hemiacetal structure has major implications on stability, reactivity, and conjugation chemistry of oxidized PSA. The assignment process also revealed deuterium exchange of the axial hydrogen at the 3- (methylene) position of the ring, which was in agreement with the literature.

## INTRODUCTION

Polysialic acid (PSA) is a naturally occurring negatively charged hydrophilic homopolymer of 5-*N*-acetyl neuraminic acid (Neu5Ac).[1,2] PSA comprises different capsular polysaccharides from *Neisseria meningitidis* (serogroup B) and *Escherichia coli* K1 (also termed colominic acid), as well as from *Moraxella liquefaciens* and *Pasteurella hemolytica* A2. The Neu5Ac subunits are all α(2→8) linked in these polysaccharides.[3] In contrast to these species that contain α(2→8) PSA, serogroup C capsular polysaccharides from *N. meningitidis* consist of partially *O*-acetylated α(2→9) linked Neu5Ac monomers. Polysialic acid from *E. coli* K92 and *E. coli* Bos-12 are heteropolymers of alternate units of α(2→8) to α(2→9) linked Neu5Ac molecules.[4] In addition, these sialic acid oligomers are also expressed in mammalian tissues.[5−7] In contrast to α(2→9) PSA, α(2→8) linked polysialic acid contains vicinal diol groups only at one end of the molecule. It can easily be produced from bacteria in large quantities and with predetermined physical characteristics.[8]

The α(2→8) polysialic acid has particular potential in drug delivery,[9] which is based on the attachment to proteins similar to the coupling of the well described coupling reaction with polyethylene glycol (PEGylation).[10] PSA is biodegradable, stable at physiological pH values, and can be used for coupling to therapeutic proteins, including antibodies and fragments, with short half-life to improve the pharmacokinetic properties

**Received:** September 30, 2013
**Revised:** March 10, 2014
**Published:** March 12, 2014





dx.doi.org/10.1021/bc400456g | *Bioconjugate Chem.* 2014, 25, 665−676

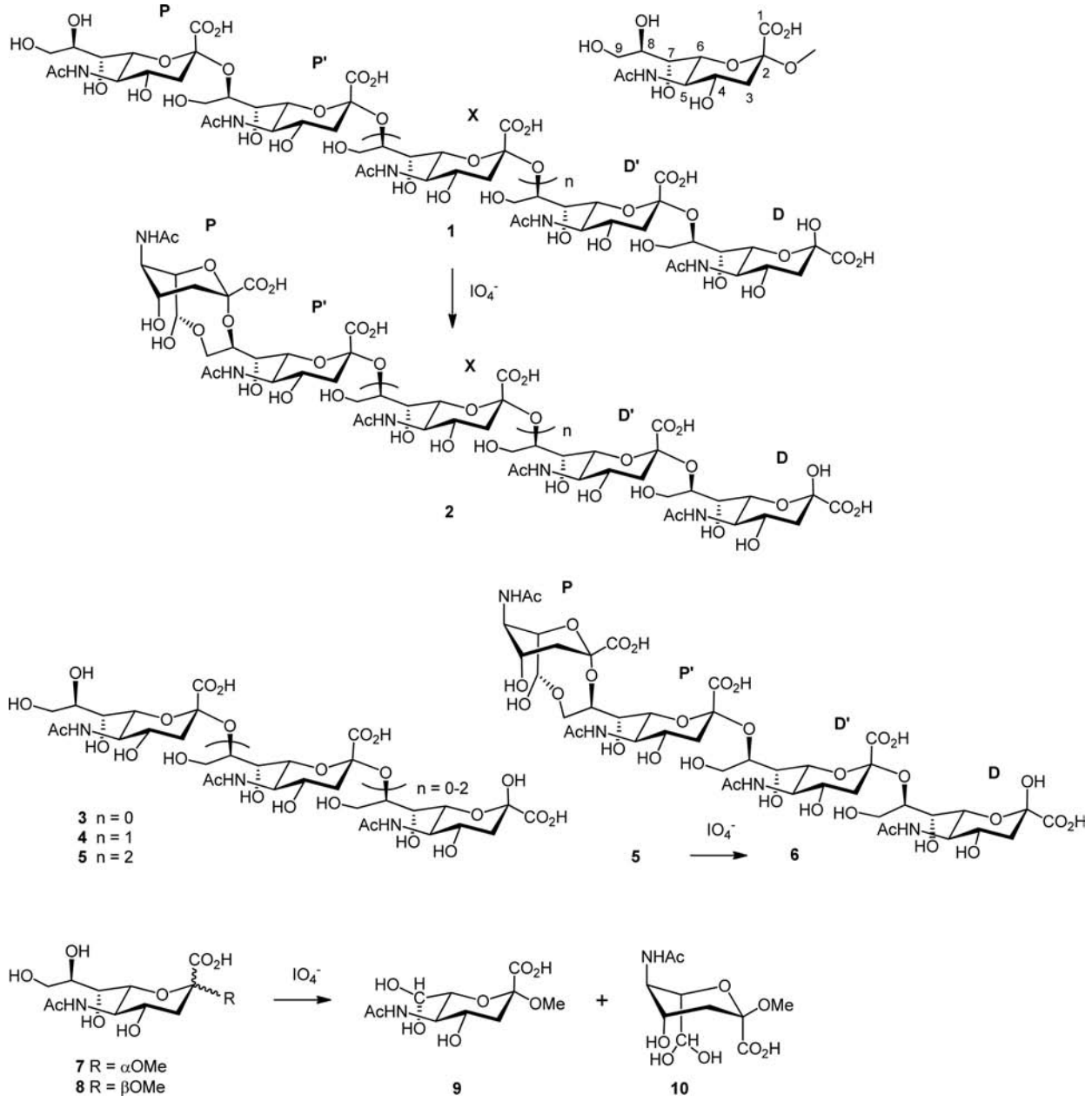


**Figure 1.** Polysialic acid, oligo- and monomeric model compounds, and their $NaIO_4$ oxidation products.

of the respective drug or biotherapeutic.[11,12] Covalent coupling of colominic acid to catalase and asparaginase has been shown to increase enzyme stability in the presence of proteolytic enzymes or blood plasma.[13,14] Comparative studies *in vivo* with polysialylated and unmodified asparaginase revealed that polysialylation can substantially increase the half-life of the enzyme.[15,16] At present, different polysialylated, improved half-life therapeutic protein preparations with PSA are in industrial development and will be brought to the market in the future. An example of a polysialylated drug is polysialylated insulin.[17]

In all cases, the key step for the coupling of PSA to a therapeutic protein is the mild oxidation of the vicinal diol groups of native PSA (natPSA) with $NaIO_4$ to form a single reactive aldehyde group, which is the basis for all further chemical reactions. The oxidation step is based on the classical Malaprade oxidation and was first described by Jennings and Lugowski.[18] The reactive terminal aldehyde group at C7 is located in a position that is accessible to selective conjugation. Examples of the potential reactions that can be used for conjugation are the coupling of oxidized PSA (oxoPSA) to amino groups of proteins directly or via reductive amination, but also to hydroxylamines, aminooxy groups, or hydrazides of functional ligands. The oxidation reaction has also been used for glycoprotein labeling and the preparation of bioconjugates.[19,20] Based on the increasing importance and acceptance of this new drug delivery technology, extensive structural data and information on native and oxidized PSA are of special interest. There are a few publications regarding the characterization of PSA focused on the assignment of the degenerate signals of the repeating units as well as conformational features.[21] Recently, on cell solution NMR using $^{13}C$ and $^{15}N$ labeled PSA has indicated a close similarity between cell-bound and purified PSA without intramolecular lactone formation.[22] No structural NMR data have been published regarding


dx.doi.org/10.1021/bc400456g | *Bioconjugate Chem.* 2014, 25, 665−676

oxoPSA and the aldehyde region of oxidized PSA, except $^{1}H$ and $^{13}C$ NMR data for the hydrated aldehyde group of the de-*O*-acetylated *N. meningitidis* serogroup C polysaccharide.[23]

Here, we report on the characterization of native and oxidized PSA by various $^{1}H$ and $^{13}C$ NMR techniques including COSY, TOCSY, HSQC, HMBC, and INADEQUATE. Starting with total assignments in spectra of oligomeric sialic acids, we were able to assign all signals due to the repeat units as well as the terminal units in the spectra of PSA and oxoPSA. Based on these findings, new structural information, especially about the chemical nature of the oxidation site in oxoPSA, was elucidated.

## RESULTS AND DISCUSSION

At the start of this investigation of the structure of oxoPSA, it was thought that an aldehyde formed at C7 of the ring that terminated the polysaccharide chain with three adjacent alcohol groups. The absence of an aldehyde resonance in either the $^{1}H$ or the $^{13}C$ spectrum of oxoPSA then led to the thought that the aldehyde had been hydrated in aqueous solution and peaks seen at 5.95 ppm ($^{1}H$) and 100.4 ppm ($^{13}C$) supported this idea. However, these chemical shifts were somewhat higher than expected for a hydrate. From a 2D NMR study, it was determined that the oxidation reaction had ultimately led to the formation of a hemiacetal between the C7 position of the terminal ring and the C9 of the penultimate ring (Structures **1** and **2** in Figure 1).

**Nomenclature.** The oxidation of PSA occurs at the ring that terminates in three adjacent alcohols. The nomenclature used in this work will refer to the ring at which oxidation will occur (in the case of PSA) or has occurred (in the case of oxoPSA) as P for proximal to the reaction site and the ring farthest away from oxidation as D for distal. The penultimate proximal and distal rings will then be referred to as P′ and D′, while P″ and D″ will denote rings twice removed from the termini, and so forth. The letter X indicates the repeat saccharide ring units that are too far from the termini to have the shifts of their peaks affected. Thus, a polysaccharide would be represented as P-P′-[X]-D′-D with the numbering system of each ring given in the inset in Figure 1. In discussing the 2D NMR data, the representation H7P − C9P′ would indicate an interaction between the proton at position 7 on the P ring and the carbon at position 9 on the P′ ring in an HMBC spectrum, while H7P−C7P would indicate a one bond interaction between the hydrogen and carbon at the 7 position in the same ring from an HSQC experiment. H3*e* and H3*a* refer to the equatorial and axial hydrogens of the ring. H9a and H9b refer to the methylene hydrogens at position 9, which are nonequivalent due to their position adjacent to a chiral carbon. In figures where the spectra are clearly due to one nucleus or the other, the ″C″ and ″H″ will be dropped from the designation.

**Spectral Assignments.** *Oligomers of Unoxidized PSA.* Early in this investigation it became clear that an accurate determination of the site of oxidation would rely on as many assignments as possible of the small resonances in the chain terminating rings. The NMR spectra of Neu5Ac, the basic repeat unit of PSA and its dimer, trimer, and tetramer (TeSA) (Structure **5** in Figure 1) were obtained. We had difficulty assigning all of the resonances in the trimer and the tetramer using the normal array of two-dimensional spectra, COSY, TOCSY, HSQC, and HMBC. The problem was that the couplings between positions 6 and 7 were small.[24−26] For the TeSA sample, we were able to identify four sets of resonances related to positions 3, 4, 5, and 6 and four sets of resonances related to positions 7, 8, and 9. The difficulty was determining which set of 3, 4, 5, and 6 resonances was in the same monomer unit with which set of 7, 8, and 9 resonances. To remove this ambiguity, $^{13}C$ INADEQUATE spectra were obtained for the trimer and tetramer, and the spectrum of the latter is shown in Figure 2. The INADEQUATE spectrum is a double quantum

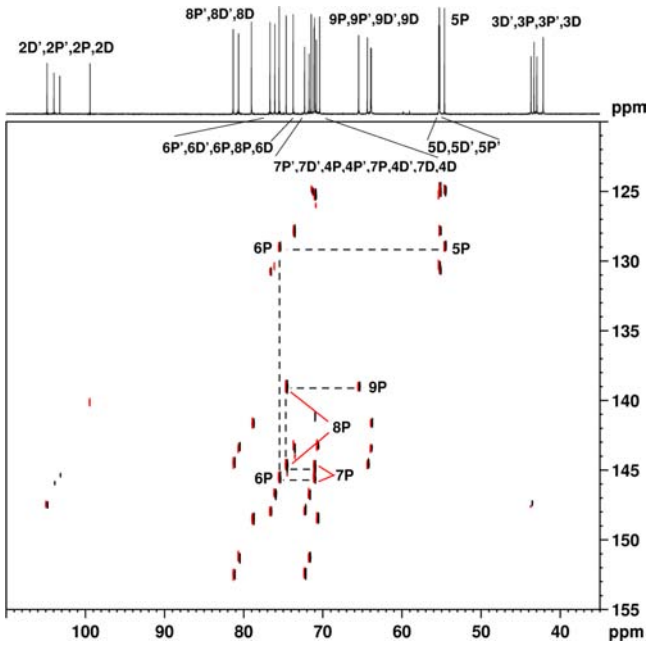


**Figure 2.** $^{13}C$ NMR INADEQUATE spectrum of TeSA where the carbon peaks occur at their normal frequencies in the directly detected dimension and at the sum of the chemical shifts of the coupled carbons in the indirect dimension. Dotted lines show a representative set of connectivities for adjacent carbons between 5P and 9P.

coherence spectrum where the correlations between adjacent carbons occur at their normal frequencies in the directly detected dimension and at the sum of the chemical shifts of the coupled carbons in the indirect dimension. The dotted lines in Figure 2 show how these data were used to make assignments for carbons between 5P and 9P. All carbon connectivities were detected for carbons 2 to 9. The resonances for C1 were determined by HMBC connectivities to the associated C3. Except for the P ring methyl, it was not possible to assign the methyl or carbonyl carbons of the *N*-acetyl groups because their resonances were highly overlapped. Chemical shifts for the acid carbonyl carbons in P, P′, D′, and D rings were determined by using connectivities to H3 resonances in these rings found in HMBC spectra. Once chemical shift offsets were accounted for, the trimer and tetramer assignments were in good agreement with the literature.[21,27−29] The differences were generally <0.1 ppm and exceptions with differences as large as 2−5 ppm appeared to be due to an interchange of assignments (see Supporting Information table).

Finally, a sample of the TeSA was oxidized to form oxoTeSA (Structure **6** in Figure 1) and complete assignments were made for this model compound as well. In parallel, periodate oxidation of both anomeric methyl glycosides of Neu5Ac (Structures **7** and **8** in Figure 1) was performed to generate data for the 7-aldehyde moiety.

*Native (Unoxidized) PSA.* The assignments of the repeat units for natPSA, which are identical for oxoPSA, are given in


dx.doi.org/10.1021/bc400456g | *Bioconjugate Chem.* 2014, 25, 665−676

Table 1. $^{1}H$ and $^{13}C$ Chemical Shifts (ppm) for the Repeat Unit in PSA

| | 1 | 2 | 3 | 4 | 5 | 6 | 7 | 8 | 9 | $\underline{CH_3}CON$ | $CH_3\underline{CON}$ |
|---|---|---|---|---|---|---|---|---|---|---|---|
| $^{13}C$ | 177.87 | 103.84 | 42.67 | 71.24 | 55.30 | 76.03 | 71.93 | 80.74 | 64.09 | 25.37 | 176.09 |
| $^{1}H$ | NA | NA | 2.69, 1.75 | 3.60 | 3.84 | 3.64 | 3.91 | 4.12 | 4.22, 3.46 | 2.11 | NA |

Table 1. Once the assignments were made for the TeSA, a comparison of its $^{13}C$ spectrum to that of the natPSA-4 kDa was made as shown in Figure 3. This allowed assignment of all of the end group peaks that were not overlapped by peaks from the repeat units. On the other hand, the $^{1}H$ spectrum of TeSA as shown in Figure 4 contains a large number of overlapped peaks; the $^{1}H$ spectrum of the natPSA is even more intractable. Only partial peak assignments could be made in the $^{1}H$ spectrum, so the approach was to make all the $^{13}C$ assignments that were possible, and to deduce the $^{1}H$ chemical shifts from 2D data sets. Although the data shown in Figures 3 and 4 are for the 4 kDa polysaccharide, the same end group peaks were seen in the 20 kDa material, just with a poorer signal-to-noise ratio.

*Oxidized TeSA and PSA-4 kDa.* It was expected that the oxidation of PSA would result in an aldehyde at C7 of the P ring. Although aldehydes are readily detected by both $^{1}H/^{13}C$ NMR near 9.5−10/200−210 ppm, no peaks were seen in the spectra of oxoTeSA or oxoPSA-4 kDa in these regions. However, treatment of an aqueous solution of oxoPSA with the reagent, Purpald,[30] which is specific for the presence of aldehydes and turns the test solution purple, confirmed that an aldehyde was present. The positive Purpald test is an indication that the hemiacetal and aldehyde forms are in equilibrium.

*Comparison of natTeSA, oxoTeSA, and oxoPSA.* Once a majority of the $^{13}C$ assignments were made based on the oligomer models, the next step in the strategy was to identify the attached protons using the edHSQC spectra, which gives the one-bond correlations and which also identifies whether the carbon is methine/methyl or methylene based on the color-coded phase of the cross-peak. Figure 5 contains a side-by-side comparison of the edHSQC spectra of oxoTeSA and oxoPSA-4 kDa to show the assignments that were made in conjunction with the 1D and TOCSY experiments. The next step in the strategy was to use the HMBC spectra to analyze longer range correlations to identify additional assignments and verify existing ones. Figure 6 is an edHSQC/HMBC overlay showing the correlations from the H3 region to the C2 through C6 regions and the assignments made to the end groups as well as to the repeat units in the case of the oxoPSA-4 kDa.

*H-D Exchange at C3.* The sample of natTeSA that was oxidized to make oxoTeSA had been in solution in $D_2O$ for several weeks, and showed no change during that time. In order to recover material for the oxidation reaction, the solution used to obtain the NMR spectra of the natTeSA was lyophilized. A portion of the recovered material was then oxidized. After the reaction, an edited HSQC spectrum of the oxoTeSA product indicated that the H3/C3 crosspeak had a phase consistent with a methine rather than a methylene (Figures 5 and 6). This was observed because the C3 methylene had only a single hydrogen attached, which indicated that during lyophilization deuterium exchange had occurred at the C3-axial position.

Exchange of C3 hydrogens has been reported[31] to occur selectively for the C3-axial hydrogen at pD = 8 at 25 °C. In this study, $^{1}H$ and $^{13}C$ NMR spectra of natTeSA before and after deuterium exchange were compared (Figure 7). The C3 carbon resonance is broad due to coupling with $^{2}H$, and both the $^{1}H$ and $^{13}C$ peaks due to the CHD group have isotope shifts to slightly lower frequencies. We attempted to repeat this exchange experiment with a sample of natPSA-4 kDa at the literature prescribed pD and temperature and found no exchange even after 5 days. However, a sample prepared at pD 11.7 did show exchange of the C3-axial hydrogen within minutes, and after 5 days the C3-equatorial hydrogen had also exchanged. These data are in agreement with the literature, wherein the rate constants of the deuterium exchange at C-3 under alkaline conditions had been determined.[32,33]

Figure 3 contains a stacked plot of natTeSA, oxoTeSA, natPSA, and oxoPSA, and Table 2 shows the chemical shifts derived from these spectra. Note the chemical shifts of natTeSA and terminal rings of natPSA were found to be within 0.02 ppm, with three exceptions that were within 0.1 ppm and, therefore, the natPSA chemical shift assignments were omitted from Table 2.

Slight differences in the chemical shifts of the oxoTeSA may be due to the fact that the data were acquired at 5 °C because the material was made *in situ* in the NMR tube and the temperature was kept low to inhibit further unwanted oxidation. Given this possibility, the peaks in the spectra of oxoTeSA and oxoPSA show a very good chemical shift agreement with only 3 peaks having a shift of greater than 0.1 ppm. The spectrum of the oxoPSA-4 kDa shows small peaks throughout the spectrum which have identical chemical shifts to the peaks in the natTeSA. Therefore, these peaks were assigned to a small unreacted fraction of natPSA-4 kDa in the sample. This was expected because measurement of the intensity of the peak at 5.95 ppm indicated that the oxidation was less than 100%. Most of the peaks at the D, D′ end of the oxidized molecules can be assigned simply by their similarity in chemical shift to the corresponding peaks in TeSA. At the P, P′ end of the molecule, there are much larger chemical shifts due to oxidation of the C7 position, and 2D spectra were required to make assignments to many of these peaks. The remaining peaks were assigned as detailed in the Supporting Information.

*Solution Stability.* As part of an ongoing accelerated stability study, 30 kDa oxoPSA samples stored as a dried powder at 2−8 °C for twelve months yielded spectra identical to those obtained for oxoPSA at the time of manufacture. However, after ∼5 days in solution, the $^{1}H$ spectra begin to show deterioration of peak at 5.9 ppm and the doublet starts to form a singlet that is shifted to slightly lower frequency (resolved at 850 MHz).

**Structure Elucidation.** *Hemiacetal Structure.* Figure 8 is an overlay of edHSQC and HMBC spectra of oxoTeSA and oxoPSA-4 kDa, which show the region critical to the assignment of the hemiacetal structure. Resonances observed at 5.95/100.4 ppm ($^{1}H/^{13}C$) were originally thought to be due to the hydrate of the C7 aldehyde, formed by oxidation of the natPSA, but the chemical shifts were not consistent with known aldehyde hydrates. The H7P peak clearly shows a multibond correlation to a resonance at 72.86 ppm, which has been assigned to C9P′, which led to the hemiacetal structure shown in Figure 1. These assignments are unambiguous because, as shown in Figure 3, all of the carbons have been accounted for in the ultimate and penultimate rings for natPSA, the natTeSA,


dx.doi.org/10.1021/bc400456g | Bioconjugate Chem. 2014, 25, 665−676

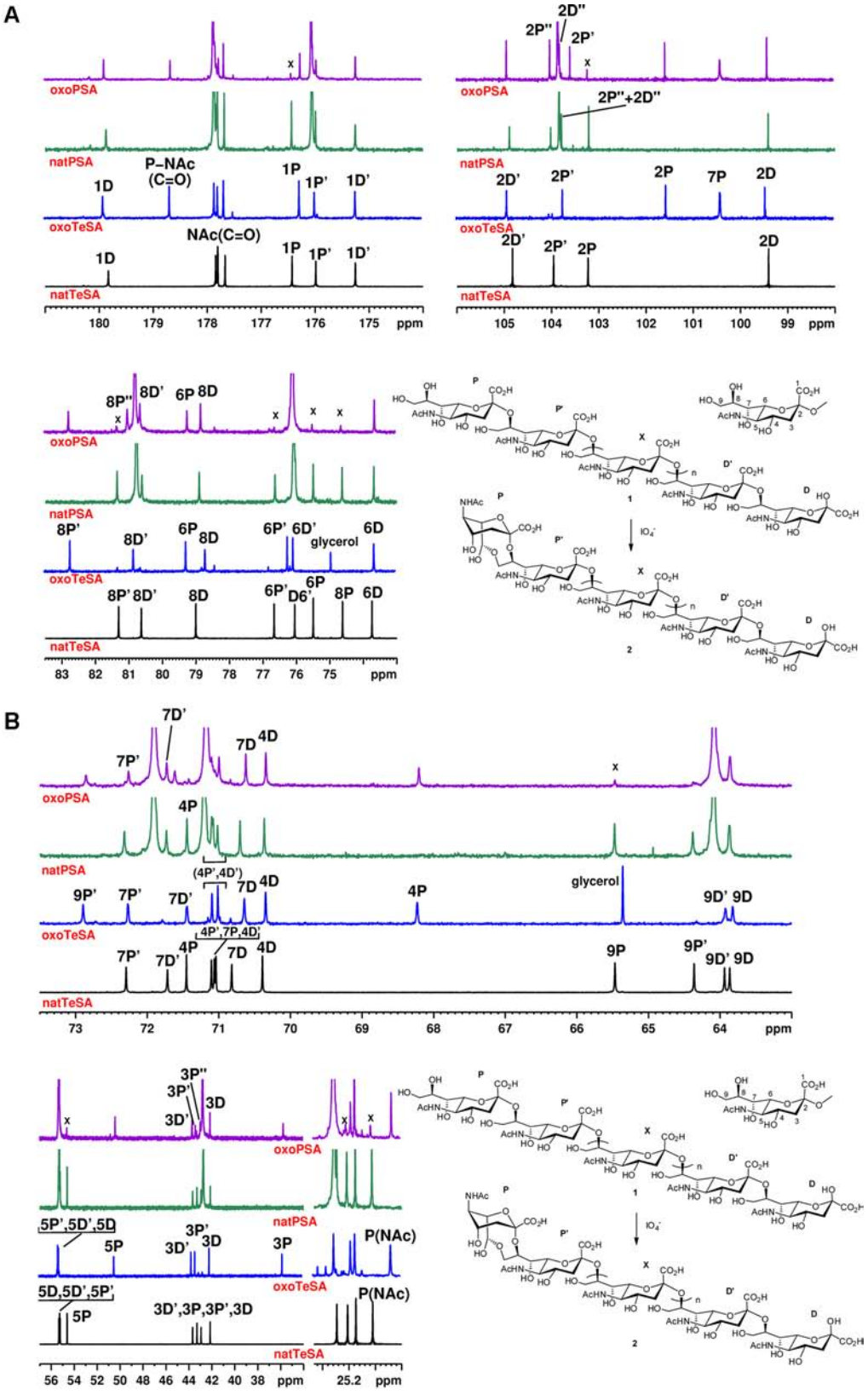


**Figure 3.** (A) $^{13}C$ NMR comparison of, from the bottom, natTeSA, oxoTeSA, natPSA-4 kDa, oxoPSA-4 kDa, expansions from 181 to 73 ppm. ″X″ denotes peaks in the spectrum of the oxoPSA that are due to residual unreacted natPSA. (B) $^{13}C$ NMR comparison of, from the bottom, natTeSA, oxoTeSA, natPSA-4 kDa, oxoPSA-4 kDa, expansions from 73.5 to 24.6 ppm. ″X″ denotes peaks in the spectrum of the oxoPSA that are due to residual unreacted natPSA.

and their related oxidation products. The chemical shift of the C9P′ peak for both the oxoTeSA and the oxoPSA-4 kDa at 72.9 ppm is about 9 ppm higher frequency than the shift of the C9P′ peak in the unreacted natTeSA, indicating its direct


dx.doi.org/10.1021/bc400456g | Bioconjugate Chem. 2014, 25, 665−676

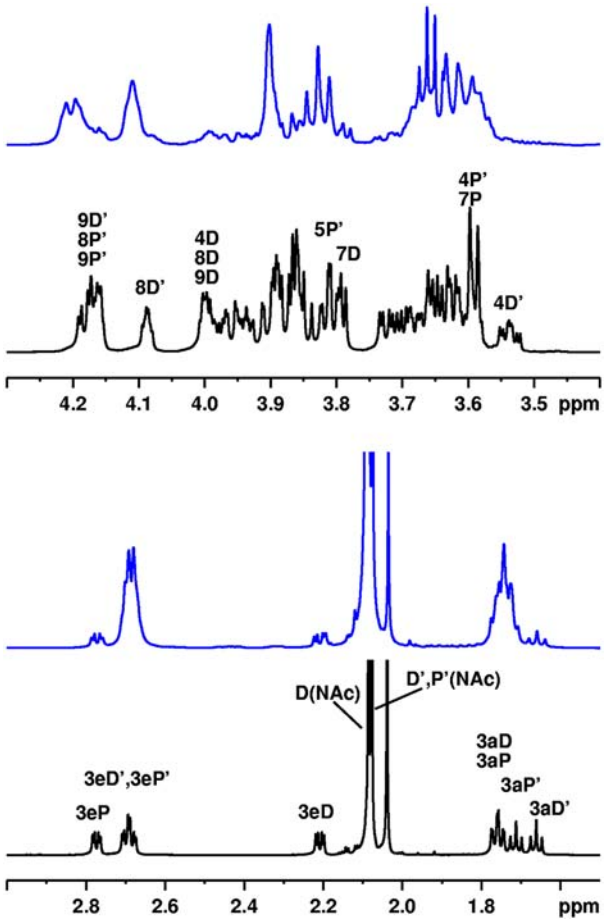


**Figure 4.** Comparison of the $^{1}$H NMR spectra of natTeSA (bottom) and natPSA-4 kDa (top). Only partial peak assignments could be made in the 4.2 to 3.5 ppm region.

involvement in a hemiacetal. The proton assignments made from the HSQC and HMBC spectra were corroborated by use of 1D TOCSY experiment. Figure 9 shows 1D TOCSY (250 ms) correlations from H7P (5.95 ppm) to all the protons in the P ring spin system (H6 to H3) for the oxoTeSA. The $J$(H7P−H6P) was measured to be 8.8 Hz. The negative peaks in this spectrum, due to their inverted phase, can be identified as through-space ROESY correlations, which can be assigned to the H9s, H8, and H7 of the P′ ring in oxoTeSA. The spectra of both the oxoTeSA and oxoPSA showed no indication of oxidation at the D ring of the molecules. HSQC, HMBC, and 1D TOCSY are the key data, along with the values of the chemical shifts that led to the determination that the oxidized site had formed a hemiacetal as shown in Figure 1, Structure **2**.

*Conformation—Oxidized Methyl Glycosides of 5N-Acetylneuraminic Acid.* Model compounds (**7** and a 2:1 $\alpha/\beta$-anomeric mixture of **7** and **8**) were subjected to mild periodate oxidation which resulted in exclusive formation of the hydrated 7-aldehyde derivatives as evidenced by correlated $^{1}$H/$^{13}$C signals at 4.97/91.53 for **9** and 5.02/91.81 ppm for **10**, respectively. Notably, the $^{1}$H NMR signals of the $\beta$-pyranoside **10** showed small values for the vicinal homonuclear coupling constants $J_{4,5}$ and $J_{5,6}$. In conjunction with the low-frequency shifts of the C-3 and C-5 carbon signals (at 35.75 and 50.91 ppm, respectively), an inversion of the chair conformation was indicated. Similar spectroscopic features have been described for related 1,7-lactone derivatives[34,35] and the 2,7-anhydro-derivative of Neu5Ac[36,37] (being present in the $^{5}C_{2}$ conformation). Furthermore, the large values of the homonuclear coupling constant $J_{6,7}$ in the 1,7-lactone and 2,7-anhydro-Neu5Ac derivatives as well as in the oxidized methyl glycoside **10**, oxoTeSA, and oxoPSA all indicate an *anti* orientation of H-6 relative to H-7. The chemical shifts of oxoTeSA and oxoPSA-4 kDa presented in Table 1 are consistent with this inverted chair conformation. Conformational studies on $\alpha(2\rightarrow8)$ linked disialosides by molecular dynamics revealed substantial flexibility of the conformations around the C7−C8 and C6−C7 bonds of the penultimate unit and a water-mediated inter-residue hydrogen-bond interaction between O7 at the terminal end and O9 of the adjacent unit.[38,39]

## CONCLUSIONS

Periodate oxidation of monomeric methyl glycosides yielded the expected 7-hydrated aldehyde forms. Through the use of multiple one- and two-dimensional NMR experiments applied to tri- and tetrasialic acid oligomers as well as to 4 and 20 kDa oxidized polysialic acid, we have made full peak assignments and demonstrated that the major product formed with the sodium periodate oxidation of polysialic acid is a hemiacetal between C7 of the terminal unit at the P ring of the chain and the C9 position of the penultimate ring, P′, in the chain. Furthermore, no oxidation was detected at the D ring in spectra of oxoTeSA and oxoPSA. This leaves only one site on the PSA available for conjugation, resulting in a discrete monomeric protein product. The existence of the hemiacetal structure at the P ring of oxoPSA used for drug conjugation has major implications on its stability, reactivity, and conjugation chemistry with therapeutic proteins. This characterization is important for development of new and next-generation protein drug products.

## EXPERIMENTAL PROCEDURES

**Samples.** This work was initiated with samples of PSA natPSA and oxoPSA, which had an average molecular weight of 20 kDa. The mass of a sialic acid repeat unit is 291.25 Da giving about 69 repeat units per chain. This meant that the end group resonances were only ∼1.5% of the repeat unit signals and created a problem in both the signal-to-noise of these resonances and overlap by the very large resonances due to the repeat units. Samples of nat- and oxoPSA with a lower MW were investigated next.

From the $^{1}$H NMR spectrum of the lower MW oxoPSA (see Figure 4), peaks due to the H3P (2.8 ppm) and H3D (2.2 ppm) hydrogens are well resolved and can be used to estimate the intensity of the end group, while the peaks near 2.7 ppm represent the remainder of the equatorial peaks in the material. These peaks were used to estimate that the MW of the material was actually about 3−4 kDa (see Supporting Information for details). For simplicity, this material will be referred to as PSA-4 kDa. From the spectrum of the oxoPSA one can see small peaks throughout the spectrum that coincide with the chemical shifts of the peaks in natTeSA and therefore represent unoxidized PSA. From the relative intensities of these small peaks, one can deduce that oxidation of PSA was only about 90% complete.

The lower MW of these materials meant that the repeat units per chain were about 14 and the end groups were closer to 7% of the total repeat units. These materials gave the identical peaks that were seen in the 20 kDa materials, but spectra with


dx.doi.org/10.1021/bc400456g | *Bioconjugate Chem.* 2014, 25, 665−676

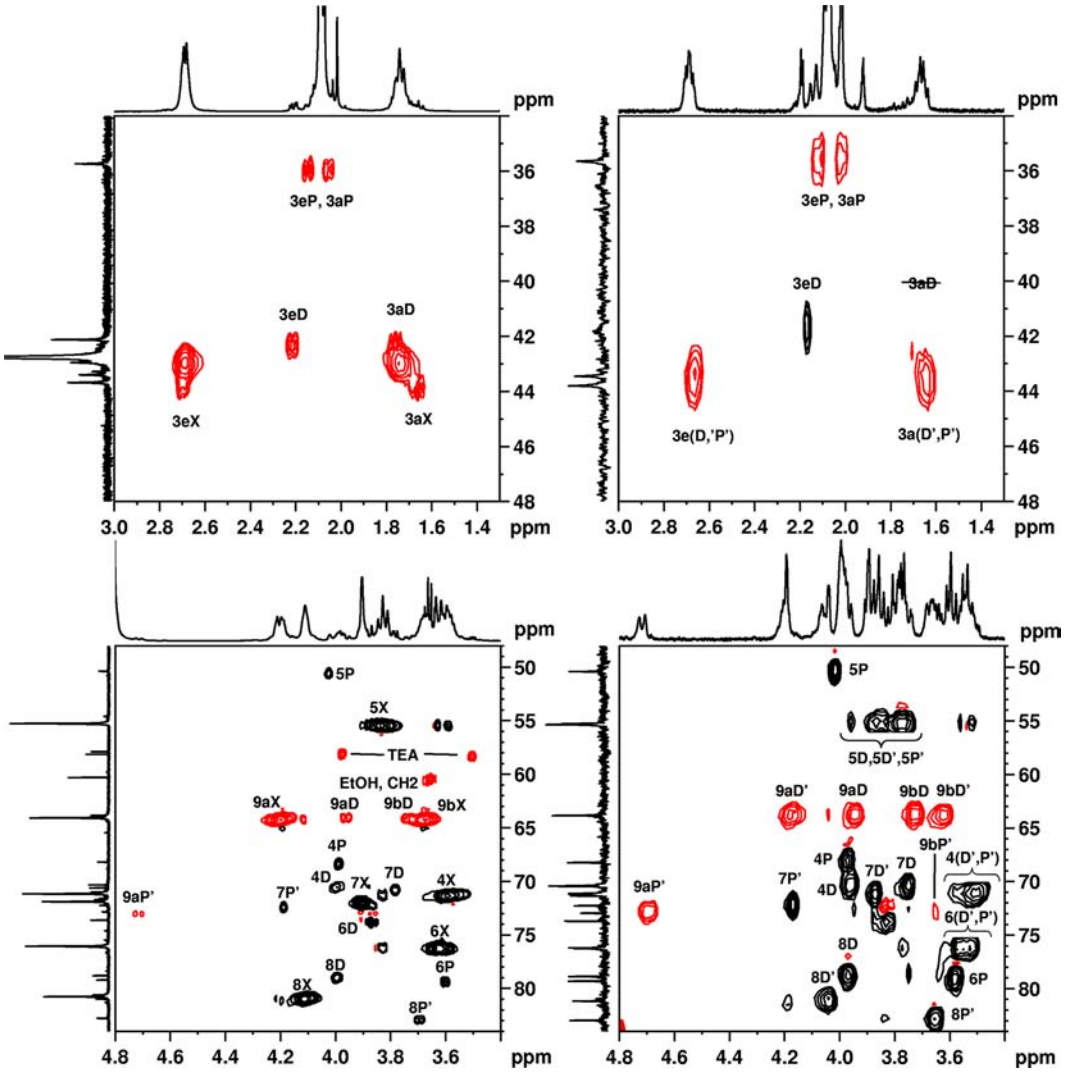


**Figure 5.** HSQC spectra and assignments for oxoPSA-4 kDa (left panels) and oxoTeSA (right panels). Top panels show the H3/C3 region; bottom panels show the H/C region for positions 4 to 9. TEA = triethanolammonium ion. Black contours indicate $CH/CH_3$ and red contours indicate $CH_2$.

much higher signal-to-noise ratios for the small peaks due to the end groups. Finally, we investigated monomers, dimer, trimer, and tetramer of PSA.

**NMR.** NMR spectra of the monosaccharide derivatives were recorded at 27 °C in 99.9% $D_2O$ (0.6 mL) with a Bruker Avance III 600 spectrometer ($^1H$ at 600.13 MHz and $^{13}C$ at 150.9 MHz) equipped with a BBFO broad-band inverse probe head and *z*-gradients using standard Bruker NMR software. COSY experiments were recorded using the program cosygpqf with 2048 × 256 data points and 8 scans, respectively, per $t_1$-increment. HSQC spectra were recorded using hsqcedetgp with 2048 × 256 data points and 32 scans, respectively, per $t_1$-increment. HMBC spectra were measured using the hmbcgpndqf pulse program with 4096 × 128 data points and 48 scans, respectively, and spectral widths of 10.0 ppm for $^1H$ and 210 ppm for $^{13}C$.

All other NMR spectra were obtained on either a Bruker Avance III 600 (AV600) or Avance III 850 (AV850) spectrometer operating at 150.9 and 213.8 MHz, respectively, on the $^{13}C$ channels. The AV600 system was equipped with a dual ($^1H/^{13}C$) cryogenic probe, and the AV850 was equipped with a quadruple resonance inverse detection ($^1H/^{13}C/^{15}N/^{31}P$ QCI) cryogenic probe. All spectra were obtained at 25 °C, except that spectra of oxoTeSA were obtained at 5 °C. Typical survey conditions were used to obtain the 1D data sets and employed a typical delay-pulse-acquire sequence, referred to as Bruker zg ($^1H$) or zgig ($^{13}C$) pulse sequences, where the ig refers to inverse gating of the decoupler to turn it on only during acquisition. For $^1H$ spectra, data were acquired with a spectral window of 12 ppm, 65k data points, a 90° pulse width, 8 scans, and an interpulse delay of 30 s; for $^{13}C$ spectra, data were acquired with a spectral window of 240 ppm, 65k data points, a 90° pulse width, 1000 to 30,000 scans, an interpulse delay of 1s, and broadband decoupling during the acquisition time only. The 1D TOCSY data were acquired using the Bruker selmlgp pulse sequence, which uses the MLEV17[40] sequence for mixing and selective refocusing with a shaped pulse. Mixing times for the 1D TOCSY experiments were 120 and 250 ms. Data were processed with either a 0.3 ($^1H$) or 3 Hz ($^{13}C$) line broadening and zero-filled one time. Unless otherwise noted, $^1H$ and $^{13}C$ chemical shifts were referenced to trimethylsilylpropionic acid-2,2,3,3 $d_4$.

Two-dimensional spectra (COSY,[41] TOCSY,[40] edited-HSQC (edHSQC),[42] and HMBC[43]) were obtained with 2k and 128 or 256 data points, in the f2 and f1 dimensions, respectively. The *J* value for the HSQC and HMBC


dx.doi.org/10.1021/bc400456g | *Bioconjugate Chem.* 2014, 25, 665−676

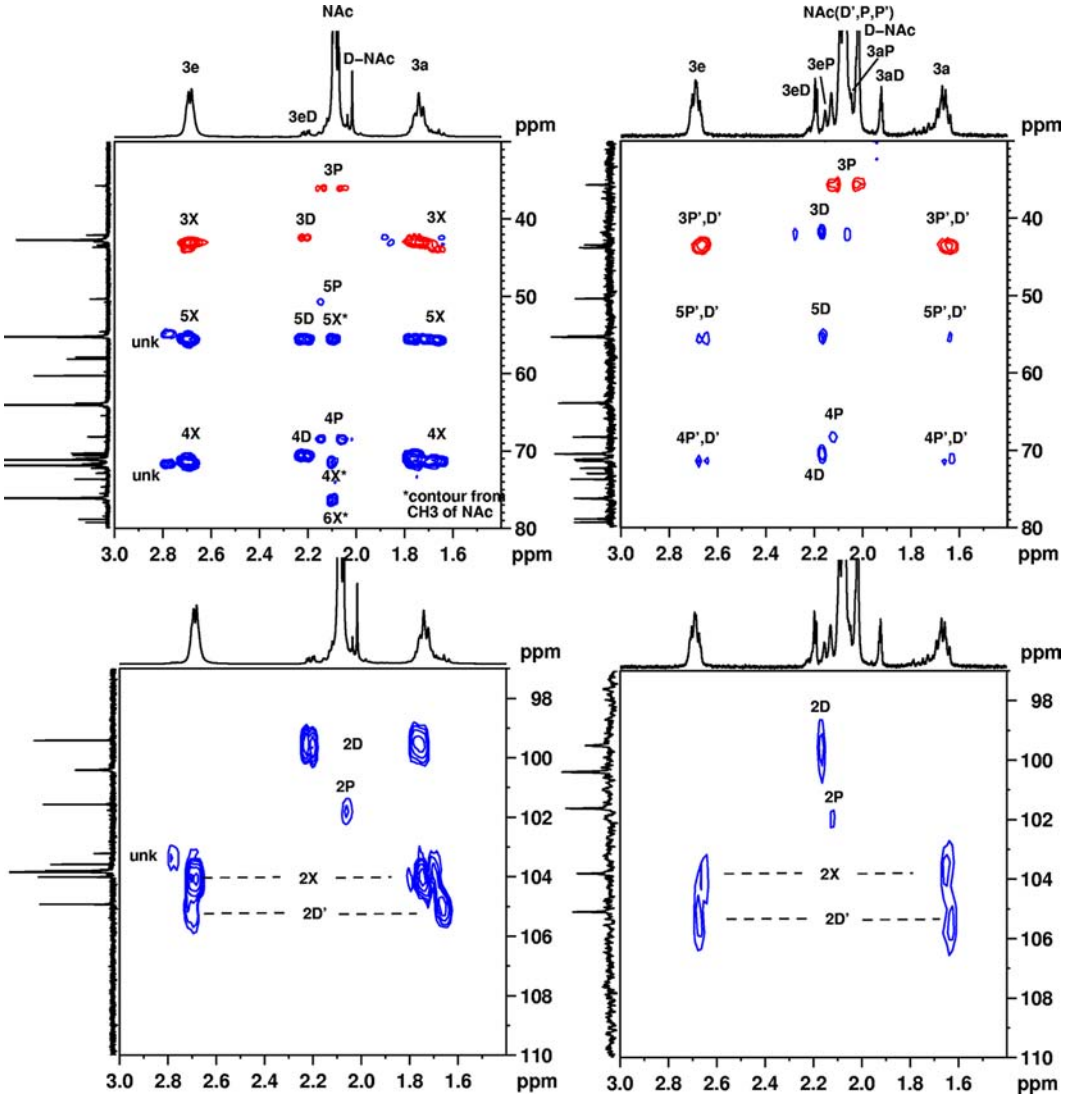


**Figure 6.** 2D spectra with assignments for H3 resonances of oxoPSA-4 kDa (left panels) and oxoTeSA (right panels). Top panels are overlays of HSQC (black contours indicate CH/$CH_3$ and red contours indicate $CH_2$) and HMBC (blue) of the C3−C6 region; bottom panels show the C2 region of the HMBC.

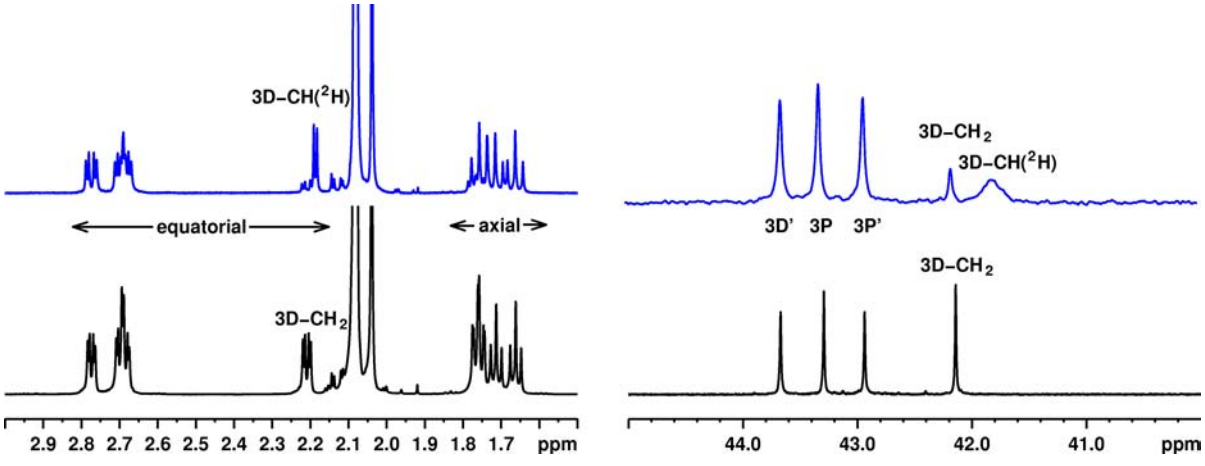


**Figure 7.** $^{1}H$ (left) and $^{13}C$ (right) NMR spectra of natTeSA before (bottom) and after (top) deuterium exchange.

experiments was 145 Hz for 1-bond couplings and 5 Hz for long-range couplings. Data were processed using a squared sine-bell and zero filling one time in the f1 dimension. INADEQUATE[44] spectra were obtained in a similar manner, except the number of data points in the f2 dimension was 8k.


dx.doi.org/10.1021/bc400456g | Bioconjugate Chem. 2014, 25, 665−676

Table 2. $^{1}H$ and $^{13}C$ NMR End Group Chemical Shifts of TeSA, oxoTeSA, and oxoPSA-4 kDa[a]

| TeSA | | | | oxoTeSA | | | | oxoPSA-4 kDa | | | |
|---|---|---|---|---|---|---|---|---|---|---|---|
| no | ring | $^{13}C$ | $^{1}H$ | no | ring | $^{13}C$ | $^{1}H$ | no | ring | $^{13}C$ | $^{1}H$ |
| 1 | D | 179.84 | NA | 1 | D | 179.92 | NA | 1 | D | 179.89 | NA |
| 2 | D | 99.40 | NA | 2 | D | 99.45 | NA | 2 | D | 99.41 | NA |
| 3a | D | 42.14 | 1.762 | 3a | D | 42.12 | NA | 3a | D | 42.11 | 1.76 |
| 3e | D | | 2.21 | 3e | D | | 2.18 | 3e | D | | 2.21 |
| 4 | D | 70.39 | 4.00 | 4 | D | 70.35 | 3.98 | 4 | D | 70.34 | 3.99 |
| 5 | D | 55.23 | 3.87 | 5 | D | 55.32 | 3.8 | 5 | D | 55.20 | 3.87 |
| 6 | D | 73.73 | 3.87 | 6 | D | 73.65 | 3.83 | 6 | D | 73.63 | 3.87 |
| 7 | D | 70.80 | 3.79 | 7 | D | 70.65 | 3.76 | 7 | D | 70.62 | 3.78 |
| 8 | D | 79.00 | 4.00 | 8 | D | 78.69 | 3.97 | 8 | D | 78.82 | 3.99 |
| 9a | D | 63.87 | 4.00 | 9a | D | 63.83 | 3.96 | 9a | D | 63.86 | 3.96 |
| 9b | D | | 3.72 | 9b | D | | 3.73 | 9b | D | | 3.76 |
| 1 | D′ | 175.25 | NA | 1 | D′ | 175.23 | NA | 1 | D′ | 175.23 | NA |
| 2 | D′ | 104.84 | NA | 2 | D′ | 104.92 | NA | 2 | D′ | 104.93 | NA |
| 3a | D′ | 43.68 | 1.662 | 3a | D′ | 43.70 | 1.65 | 3a | D′ | 43.68 | 1.66 |
| 3e | D′ | | 2.70 | 3e | D′ | | 2.68 | 3e | D′ | | 2.69 |
| 4 | D′ | 71.04 | 3.54 | 4 | D′ | 71.01 | 3.6 | 4 | D′ | 71.00 | 3.59 |
| 5 | D′ | 55.27 | 3.80 | 5 | D′ | 55.29 | 3.8 | 5 | D′ | 55.25 | 3.8 |
| 6 | D′ | 76.06 | 3.60 | 6 | D′ | 76.06 | 3.56- 3.52 | 6 | D′ | ~76[b] | 3.83 |
| 7 | D′ | 71.71 | 3.89 | 7 | D′ | 71.45 | 3.88 | 7 | D′ | 71.73 | 3.9 |
| 8 | D′ | 80.64 | 4.09 | 8 | D′ | 80.83 | 4.04 | 8 | D′ | 80.63 | 4.11 |
| 9a | D′ | 63.94 | 4.16 | 9a | D′ | 63.93 | 4.18 | 9a | D′ | 63.86 | 4.26 to 4.15 |
| 9b | D′ | | 3.65 | 9b | D′ | | 3.63 | 9b | D′ | | 3.72 to 3.63 |
| 1 | P′ | 175.99 | NA | 1 | P′ | 175.99 | NA | 1 | P′ | 175.96 | NA |
| 2 | P′ | 103.96 | NA | 2 | P′ | 103.74 | NA | 2 | P′ | 103.58 | NA |
| 3a | P′ | 42.95 | 1.712 | 3a | P′ | 43.37 | 1.65 | 3a | P′ | 43.40 | 1.71 |
| 3e | P′ | | 2.68 | 3e | P′ | | 2.68 | 3e | P′ | | 2.69 |
| 4 | P′ | 71.10 | 3.59 | 4 | P′ | 71.10 | 3.5 | 4 | P′ | 71.10 | 3.59 |
| 5 | P′ | 55.34 | 3.81 | 5 | P′ | 55.25 | 3.8 | 5 | P′ | 55.33 | 3.82 |
| 6 | P′ | 76.67 | 3.62 | 6 | P′ | 76.66 | 3.56- 3.52 | 6 | P′ | 76.17 | nd |
| 7 | P′ | 72.29 | 3.86 | 7 | P′ | 72.27 | 4.19 | 7 | P′ | 72.26 | 4.18 |
| 8 | P′ | 81.31 | 4.16 | 8 | P′ | 82.72 | 3.71 | 8 | P′ | 82.76 | 3.69 |
| 9a | P′ | 64.14 | 4.15 | 9a | P′ | 72.90 | 4.70 | 9a | P′ | 72.86 | 4.71 |
| 9b | P′ | | 3.68 | 9b | P′ | | 3.85 | 9b | P′ | | 3.85 |
| 1 | P | 176.43 | NA | 1 | P | 176.27 | NA | 1 | P | 176.26 | NA |
| 2 | P | 103.23 | NA | 2 | P | 101.55 | NA | 2 | P | 101.57 | NA |
| 3a | P | 43.30 | 1.762 | 3a | P | 35.76 | 2.03 | 3a | P | 35.75 | 2.05 |
| 3e | P | | 2.77 | 3e | P | | 2.13 | 3e | P | | 2.14 |
| 4 | P | 71.45 | 3.67 | 4 | P | 68.23 | 3.98 | 4 | P | 68.22 | 3.98 |
| 5 | P | 54.62 | 3.85 | 5 | P | 50.43 | 4.03 | 5 | P | 50.39 | 4.02 |
| 6 | P | 75.50 | 3.62 | 6 | P | 79.26 | 3.59 | 6 | P | 79.22 | 3.60 |
| 7 | P | 71.06 | 3.59 | 7 | P | 100.40 | 5.95 | 7 | P | 100.40 | 5.95 |
| 8 | P | 74.63 | 3.93 | 8 | P | NA | NA | 8 | P | NA | NA |
| 9a | P | 65.47 | 3.90 | 9a | P | NA | NA | 9a | P | NA | NA |
| 9b | P | | 3.65 | 9b | P | | NA | 9b | P | | NA |

[a]Chemical shifts given to 1 decimal place are approximations due to peak broadness. NA = Not Applicable. [b]Unresolved from the X resonance.

**Synthesis.** *Oxidized Tetrasialic Acid (oxoTeSA).* 5.1 mg of sialic acid tetramer was dissolved in 0.6 mL of acetate buffer (0.1 M, pH 5.5) and transferred to an NMR tube for analysis. (Note: The acetate buffer was prepared with acetic acid-$d_4$ and sodium acetate-$d_3$ in deuterium oxide.) Following $^{1}H$ NMR analysis, the sample was transferred to a vial containing 3.8 mg of sodium (meta)periodate to initiate the oxidation of the TeSA. Upon complete dissolution of the periodate, the sample was transferred back to an NMR tube for analysis to confirm that the reaction had occurred. NMR data were acquired on this sample for the next 48 h at 5 °C until the $^{1}H$ NMR spectrum indicated that further reactions were occurring.

*Oxidation of methyl α-Neu5Ac Glycoside 7.* Sodium metaperiodate (13 mg, 0.062 mmol) was dissolved in a solution of 1 M deuterated sodium acetate buffer (0.6 mL, pH 5.5) in an NMR tube. Methyl α-*N*-acetyl-neuraminic acid glycoside **7** (Toronto Research, 10 mg, 0.031 mmol) was added, dissolved, and subjected to NMR measurements. The first $^{1}H$ NMR spectrum obtained after 5 min at 300 K indicated complete conversion to aldehyde derivative **9**. $^{1}H$ NMR (600 MHz, $D_2O$, DSS): $\delta$ 8.43 (s, 1H, HCO), 4.97 (d, 1H, $J_{7,6}$ 1.2 Hz, H-7), 4.72 [s, 2H, $CH_2(OH)_2$] 3.76 (dd, 1H, $J_{5,6}$ 10.2 Hz, H-6), 3.72 (dd, 1H, $J_{5,4}$ 9.8 Hz, H-5), 3.58 (ddd, 1H, $J_{4,3a}$ 11.7, $J_{4,3e}$ 4.0 Hz, H-4), 3.33 (s, 3H, OMe), 2.59 (ddd, 1H, $J_{3a,3e}$ 12.4 Hz, H-3*e*), 1.89 (s, 3H, NHAc), 1.60 (t, 1H, H-3*a*). $^{13}C$ NMR


dx.doi.org/10.1021/bc400456g | *Bioconjugate Chem.* 2014, 25, 665−676

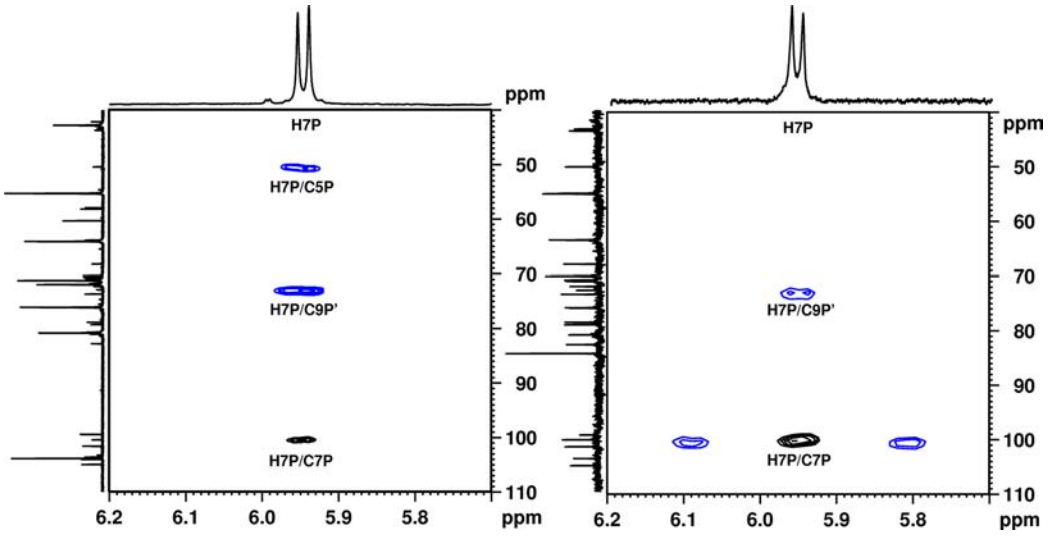


**Figure 8.** Overlaid HSQC (black) and HMBC (blue) spectra with assignments for oxoPSA-4 kDa (left panel) and oxoTeSA (right panel) for the H7 region.

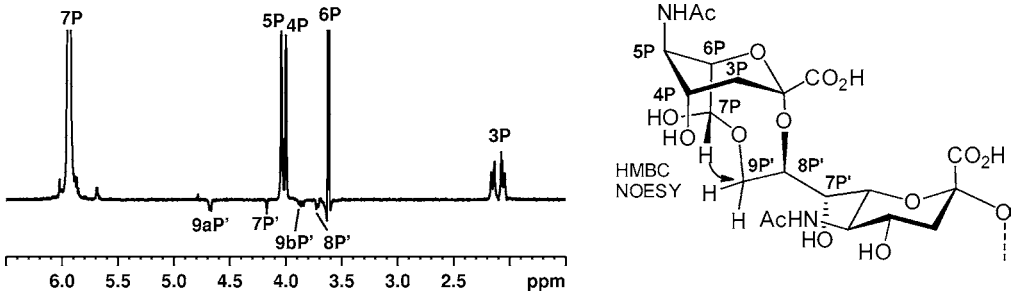


**Figure 9.** 1D TOCSY (250 ms) correlations from H7P (5.95 ppm) for oxoTeSA. Negative peaks are due to NOESY correlations.

(150 MHz, $D_2O$): $\delta$ 177.55 (NHC═O), 176.86 (OC═O), 104.22 (C-2), 91.53 (C-7), 78.57 (C-6), 70.44 (C-4), 55.38 (C-5), 54.57 ($OCH_3$), 42.83 (C-3), and 25.03 ($CH_3CO$).

*Oxidation of the Anomeric Mixture.* A solution of **7** and **8**, the methyl glycosides of the 5*N*-acetyl-neuraminic acid (11 mg, 0.034 mmol, Sigma Aldrich, $\alpha/\beta$ ratio ~2:1), was dissolved in 0.1 M sodium acetate buffer (0.5 mL; pH 5) and cooled to 0 °C. Sodium metaperiodate (5.95 mg, 0.028 mmol) was dissolved in water (0.1 mL) and added to the reaction mixture. The solution was stirred for 10 min with exclusion of light and stopped by addition of 3% aq. ethylene glycol (0.07 mL). The solution was kept overnight at 4 °C and passed over a column of BioGel-P2 (40 × 1 cm) using 20:1 $H_2O$−EtOH (v/v) as eluent. Pooling of appropriate fractions and lyophilization gave a mixture of **9** and **10** (8.8 mg, 93%). $^1$H NMR spectra were referenced to 4,4-dimethyl-4-silapentane-1-sulfonic acid (DSS). $^{13}$C NMR spectra were referenced to the ethanol methyl group at 19.68 ppm. $^1$H NMR (600 MHz, $D_2O$) for **10**: $\delta$ 5.02 (d, 1H, $J_{7,6}$ 7.4 Hz, H-7), 4.00 (br. s, 1H, H-5), 3.905 (br. dd, H-4), 3.90 (dd, 1H, $J_{5,6}$ 2.1 Hz, H-6), 3.18 (s, 3H, OMe), 1.99 (m, H-3*a*), and 1.87 (dd, 1H, $J_{3e,3a}$ 15.5, $J_{3e,4}$ 4.0 Hz, H-3*e*). $^{13}$C NMR data for **10** (150 MHz, $D_2O$): $\delta$ 178.40 (NHC═O), 176.46 (OC═O), 102.85 (C-2), 91.81 (C-7), 72.20 (C-6), 68.93 (C-4), 53.65 ($OCH_3$), 50.91 (C-5), 35.75 (C-3), and 24.55 ($CH_3CO$).

## ■ ASSOCIATED CONTENT

### Supporting Information

$^1$H and $^{13}$C NMR spectra of natTeSA before and after deuterium exchange. A table of NMR peak assignments for mono-, di-, tri-, and tetramers of sialic acid and a comparison with those available from the literature. This material is available free of charge via the Internet at http://pubs.acs.org.

## ■ AUTHOR INFORMATION

### Corresponding Author

*Phone: 1-224-270-5247. Fax: 1-224-270-2269. E-mail: christina_szabo@baxter.com.

### Notes

The authors declare no competing financial interest.

## ■ ACKNOWLEDGMENTS

The authors thank Dr. Andreas Hofinger for recording the NMR spectra of oxidized monosaccharides. The authors gratefully thank Serum Institute of India Ltd. for providing the samples of PSA and oxoPSA.

## ■ ABBREVIATIONS

PSA, polysialic acid; natPSA, native PSA; oxoPSA, oxidized PSA; TeSA, sialic acid tetramer; P, proximal ring at which oxidation occurs; D, distal ring farthest from the oxidation site; COSY, correlated spectroscopy; TOCSY, total correlated spectroscopy; NOESY, nuclear Overhauser effect spectroscopy; HSQC, heteronuclear single quantum coherence; HMBC,

heteronuclear multiple bond correlation; INADEQUATE, incredible natural abundance double quantum transfer experiment

## REFERENCES


(1) Varki, A., and Schauer, R. (2009) Sialic acids. In *Essentials of Glycobiology*, 2nd ed. (Varki, A., Cummings, R. D., Esko, J. D., Freeze, H. H., Stanley, P., Bertozzi, C. R., Hart, G. W., and Etzler, M. E., Eds) pp 197−217, Chapter 14, Cold Spring Harbor, New York.

(2) Mühlenhoff, M., Eckhardt, M., and Gerardy-Schahn, R. (1998) Polysialic acid: three dimensional structure, biosynthesis and function. *Curr. Opin. Struct. Biol. 8*, 558−564.

(3) Bhattacharjee, A. K., Jennings, H. J., Kenny, C. P., Martin, A., and Smith, I. C. (1975) Structural determination of the sialic polysaccharide antigens of *Neisseria meningitidis* serogroups B and C with carbon 13 nuclear magnetic resonance. *J. Biol. Chem. 250*, 1926−1932.

(4) Egan, W., Liu, T. Y., Dorow, D., Cohen, J. S., Robbins, J. D., Gotschlich, E. C., and Robbins, J. B. (1977) Structural studies on the sialic acid polysaccharide antigen of *Escherichia coli* strain Bos-12. *Biochemistry 16*, 3687−3692.

(5) Kiss, J. Z., and Rougon, G. (1997) Cell biology of polysialic acid. *Curr. Opin. Neurobiol. 7*, 640−646.

(6) Samuel, J., and Bertozzi, C. R. (2004) Chemical tools for the study of polysialic acid. *Trends Glycosci. Glycotechnol. 16*, 305−318.

(7) Hromatka, B. S., Drake, P. M., Kapidzic, M., Stolp, H., Goldfien, G. A., Shih, I.-M., and Fisher, S. J. (2013) Polysialic acid enhances the migration and invasion of human cytotrophoblasts. *Glycobiology 23*, 593−602.

(8) Gregoriadis, G. (1998) U.S. Patent No. 5,846,951.

(9) Gregoriadis, G., Jain, S., Papaioannou, I., and Laing, P. (2005) Improving the therapeutic efficacy of peptides and proteins: a role for polysialic acids. *Int. J. Pharm. 300*, 125−130.

(10) Roberts, M. J., Bentley, M. D., and Harris, J. M. (2002) Chemistry for peptide and protein PEGylation. *Adv. Drug Delivery Rev. 54*, 459−476.

(11) Constantinou, A., Epenetos, A. A., Hreczuk-Hirst, D., Jain, S., and Deonarain, M. P. (2008) Modulation of antibody pharmacokinetics by chemical polysialylation. *Bioconjugate Chem. 19*, 643−650.

(12) Constantinou, A., Epenetos, A. A., Hreczuk-Hirst, D., Jain, S., Wright, M., Chester, K. A., and Deonarain, M. P. (2009) Site-Specific polysialylation of an antitumor single-chain Fv fragment. *Bioconjugate Chem. 20*, 924−931.

(13) Gregoriadis, G., Fernandes, A., McCormack, B., Mital, M., and Zhang, X. (1999) Polysialic acids: potential role in therapeutic constructs. *Biotechn. Genet. Eng. Rev. 16*, 203−215.

(14) Gregoriadis, G., Fernandes, A., Mital, M., and McCormack, B. (2000) Polysialic acids: potential in improving the stability and pharmacokinetics of proteins and other therapeutics. *Cell. Mol. Life Sci. 57*, 1964−1969.

(15) Fernandes, A. I., and Gregoriadis, G. (1997) Polysialylated asparaginase: preparation, activity and pharmacokinetics. *Biochim. Biophys. Acta 1341*, 26−34.

(16) Fernandes, A. I., and Gregoriadis, G. (2001) The effect of polysialylation on the immunogenicity and antigenicity of asparaginase: implication in its pharmacokinetics. *Int. J. Pharm. 217*, 215−224.

(17) Jain, S., Hreczuk-Hirst, D. H., McCormack, B., Mital, M., Epenetos, A., Laing, P., and Gregoriadis, G. (2003) Polysialylated insulin: synthesis, characterization and biological activity in vivo. *Biochim. Biophys. Acta 1622*, 42−49.

(18) Jennings, H. J., and Lugowski, C. (1981) Immunochemistry of groups A, B, and C meningococcal polysaccharide-tetanus toxoid conjugates. *J. Immunol. 127*, 1011−1018.

(19) Key, J. A., Li, C., and Cairo, C. W. (2012) Detection of cellular sialic acid content using nitrobenzoxadiazole carbonyl-reactive chromophores. *Bioconjugate Chem. 23*, 363−371.

(20) Dhal, P. K., Polomoscanik, S. C., Gianolio, D. A., Starremans, P. G., Busch, M., Alving, K., Chen, B., and Miller, R. J. (2013) Well-defined aminooxy terminated *N*-(2-hydroxypropyl) methacrylamide macromers for site specific bioconjugation of glycoproteins. *Bioconjugate Chem. 24*, 865−877.

(21) Michon, F., Brisson, J. R., and Jennings, H. J. (1987) Conformational differences between linear $\alpha$ (2−8)-linked homosialooligosaccharides and the epitope of the group B meningococcal polysaccharide. *Biochemistry 26*, 8399−8405.

(22) Azurmendi, H. F., Vionnet, J., Wrightson, L., Trinh, L. B., Shiloach, J., and Freedberg, D. I. (2007) Extracellular structure of polysialic acid explored by on cell solution NMR. *Proc. Natl. Acad. Sci. U.S.A. 104*, 11557−11561.

(23) Jones, C., and Lemercinier, X. (2002) Use and validation of NMR assays for the identity and *O*-acetyl content of capsular polysaccharides from *Neisseria meningitides* used in vaccine manufacture. *J. Pharm. Biomed. Anal. 30*, 1233−1247.

(24) Yamasaki, R., and Bacon, B. (1991) Three-dimensional structural analysis of the group B polysaccharide of *Neisseria meningitidis* 6275 by two-dimensional NMR: the polysaccharide is suggested to exist in helical conformations in solution. *Biochemistry 30*, 851−857.

(25) Baumann, H., Brisson, J. R., Michon, F., Pon, R., and Jennings, H. J. (1993) Comparison of the conformation of $\alpha$(2−8) polysialic acid with its reduced and *N*-acyl derivatives. *Biochemistry 32*, 4007−4013.

(26) Prytulla, S., Lambert, J., Lauterwein, J., Klessinger, M., and Thiem, J. (1990) Configurational assignment in *N*-acetylneuraminic acid and analogs via the geminal C,H coupling constants. *Magn. Reson. Chem. 28*, 888−901.

(27) Eckert, T., Lu, C. P., Chen, C. S., Wu, S. H., and Gervay-Hague, J. (2011) NMR studies of the reversible and regioselective lactonization of $\alpha$-2,8-linked trisialic acid in aqueous acid. *Tetrahedron Lett. 52*, 2250−2253.

(28) Yongye, A. B., Gonzalez-Outeirino, J., Glushka, J., Schultheis, V., and Woods, R. J. (2008) The conformational properties of methyl $\alpha$-(2,8)-di/trisialosides and their *N*-Acyl analogues: implications for anti-*Neisseria meningitidis* B vaccine design. *Biochemistry 47*, 12493−12514.

(29) Battistel, M. D., Shangold, M., Trinh, L., Shiloach, J., and Freedberg, D. I. (2012) Evidence for helical structure in a tetramer of $\alpha$2−8 sialic acid: unveiling a structural antigen. *J. Am. Chem. Soc. 134*, 10717−10720.

(30) Quesenberry, M. S., and Lee, Y. C. (1996) A rapid formaldehyde assay using purpald reagent: application under periodation conditions. *Anal. Biochem. 234*, 50−55.

(31) Klepach, T., Carmichael, I., and Serianni, A. S. (2008) $^{13}$C-labeled N-acetyl-neuraminic acid in aqueous solution: detection and quantification of acyclic keto, keto hydrate, and enol forms by $^{13}$C NMR spectroscopy. *J. Am. Chem. Soc. 130*, 11892−11900.

(32) Friebolin, H., Schmidt, H., and Supp, M. (1981) $^{1}$H-NMR-Untersuchungen an Sialinsäuren. Markierung von N-Acetyl-D-Neuraminsäure mit Deuterium. *Tetrahedron Lett. 22*, 5171−5174.

(33) Schmidt, H., and Friebolin, H. (1983) $^{1}$H-NMR- Untersuchungen an Sialinsäuren, IV Kinetik und Mechanismus des Austauschs von Protonen an C-3 der N-Acetyl-D-Neuraminsäure gegen Deuterium oder Tritium. *J. Carbohydr. Chem. 2*, 405−413.

(34) Allevi, P., Anastasia, M., Costa, M. L., and Rota, P. (2011) Two procedures for the syntheses of labeled sialic acids and their 1,7-lactones. *Tetrahedron: Asymmetry. 22*, 338−344.

(35) Colombo, R., Anastasia, M., Rota, P., and Allevi, P. (2008) The first synthesis of N-acetylneuraminic acid 1,7-lactone. *Chem. Commun. 43*, 5517−5519.

(36) Furuhata, K., and Ogura, H. (1992) Synthesis of 2,7-anhydrosialic acid. *Chem. Pharm. Bull. 40*, 3197−3200.

(37) Li, Y. T., Nakagawa, H., Ross, S. A., Hansson, G. C., and Li, S. C. (1990) A novel sialidase which releases 2,7-anhydro-$\alpha$-*N*-acetylneuraminic acid from sialoglycoconjugates. *J. Biol. Chem. 265*, 21629−21633.

(38) Suresh, M. X., and Veluraja, K. (2003) Conformations of terminal sialyloligosaccharide fragments − a molecular dynamics study. *J. Theor. Biol. 222*, 389−402.

(39) Vasudevan, S. V., and Balaji, P. V. (2002) Molecular dynamics simulations of α 2−8-linked disialoside: conformational analysis and implications for binding to proteins. *Biopolymers 63*, 168−180.
(40) Bax, A., and Davis, D. G. (1985) MLEV-17-based two-dimensional homonuclear magnetization transfer spectroscopy. *J. Magn. Reson. 65*, 355−360.
(41) Hurd, R. E. (1990) Gradient-enhanced spectroscopy. *J. Magn. Reson. 87*, 422−428.
(42) Boyer, R. D., Johnson, R., and Krishnamurthy, K. (2003) Compensation of refocusing inefficiency with synchronized inversion sweep (CRISIS) in multiplicity-edited HSQC. *J. Magn. Reson. 165*, 253−259.
(43) Meissner, A., Moskau, D., Neilson, N. C., and Sørensen, O. W. (1997) Proton-detected $^{13}C$-$^{13}C$ double quantum coherence. *J. Magn. Reson. 124*, 245−249.
(44) Bourdonneau, M., and Ancian, B. (1998) Rapid-pulsing artifact-free double-quantum-filtered homonuclear spectroscopy. The 2D-INADEQUATE experiment revisited. *J. Magn. Reson. 132*, 316−327.